Bulgarian Journal of Physics vol. **46** (2019) 424–433

Shape Phase Transition, Shape Coexistence and Mixing Phenomena within the Bohr Model

P. Buganu[1], **R. Budaca**[1,2], **A. Lahbas**[3,4], **A.I. Budaca**[1]
[1]Department of Theoretical Physics, National Institute for Physics and Nuclear Engineering, Str. Reactorului 30, RO-077125, POB-MG6, Bucharest-Măgurele, Romania
[2]Academy of Romanian Scientists, 54 Splaiul Independentei, Bucharest, RO-050094, Romania
[3]ESMaR, Department of Physics, Faculty of Sciences, Mohammed V University in Rabat, Morocco
[4]LPHEA, Department of Physics, Faculty of Sciences Semlalia, Cadi Ayyad University, Marrakesh, Morocco

Abstract. Two methods of solving the Bohr Hamiltonian with sextic oscillator potential in the β variable are presented, namely a quasi-exact method involving polynomials and a numerical diagonalization in a basis of Bessel functions of the first kind. The formalisms are used to describe shape phase transitions and critical points, respectively shape coexistence and mixing phenomena in nuclei.

KEY WORDS: Bohr model, Sextic potential, Shape phase transitions and critical points, Shape coexistence and mixing phenomena.

1 Introduction

The Bohr model [1, 2] describes the low-lying spectra of nuclei in terms of vibrations and rotations of their ground state shape, being an appropriate model to investigate shape phase transitions [3–5] and critical points [6, 7], respectively shape coexistence and mixing phenomena [8]. Until recently, the studies involving the Bohr Hamiltonian were focused more on the understanding of the shape phase transitions and their critical points [9, 10], while in the last two years, a new direction of its application has been proposed, namely for shape coexistence and mixing phenomena [11]. The idea is based on the introduction of a barrier which separates two configurations of states, one associated with a spherical minimum, while the other one with a deformed minimum. By controlling the height of this barrier, one can have shape coexistence and mixing phenomena [12] or shape fluctuations specific for the critical point of a shape phase transition when the height is close to zero. Such behavior could be reproduced by a sextic anharmonic oscillator potential in the β variable [11], which depending on its parameters, can exhibit a single spherical minimum or a deformed

one, respectively simultaneous spherical and deformed minima separated by a barrier. The sextic potential has been used for the first time for the Bohr Hamiltonian to describe γ-unstable nuclei [13, 14], by applying a quasi-exactly solvable method [15] to get analytical expressions for energies and wave functions. The same method has been used then for triaxial and prolate shapes [16, 17], respectively for their γ-rigid analogs [18, 19]. All these solutions have been written in an unified equation, by showing the similarity, as well as the difference between them, but also by underling the importance of the solvability order on the structure of the states, especially in the critical point [20]. This latter aspect, has been recently investigated more carefully within the phase transition from spherical vibrator to γ-unstable shape [21]. More details about these results, are presented in the next sections. The quasi-exactly solvable method has the advantage of offering analytical expressions for the eigenvalues and eigenfunctions, but in the same time, it comes with some constraints for the parameters defining the potential which restrict the range of its applications. For example, the quasi-exactly solvable sextic potential cannot be applied to describe shape coexistence and mixing phenomena and that because the barrier which separates the two minima cannot be adequately introduced in this case [19]. Because of that, the Bohr Hamiltonian is solved in Ref. [11] for a more general sextic potential by numerical diagonalization in a basis of Bessel functions of the first kind, which in turn are solutions of the same equation but for an infinite square well potential. This numerical method has been already applied with success for experimental data by evidencing shape coexistence and mixing in ^{76}Kr [12], ^{72,74,76}Se [22] and ^{96,98,100}Mo [23] nuclei.

The plan of the present work is the following. In Section 2, the two methods of solving the Bohr Hamiltonian with sextic potential, the quasi-exact and numerical one, are briefly presented, while in Section 3 are shown and discussed recent results and applications of these methods. Section 4 is dedicated for the main achievements and possible new developments of the model.

2 Bohr Hamiltonian with a Sextic Potential

The β part of the Bohr Hamiltonian equation can be written as [9]

$$\left[-\frac{d^2}{d\beta^2}+\frac{\omega}{\beta^2}+u(\beta)\right]\phi(\beta)=\varepsilon\phi(\beta), \tag{1}$$

where ω is based in general on the γ-axial deformation. For the cases discussed in the present study, one has $\omega=(\tau+1)(\tau+2)$ for γ-unstable, respectively $[L(L+1)/3]+2$ for prolate shape. The expression for the eigenvalue ε depends on the choice of the potential $u(\beta)$, but also on the solving method. In what follows, the sextic oscillator potential is considered involving a quasi-exactly solvable method [15], respectively a numerical one [11].

2.1 Quasi-exactly solvable method

In this case, the sextic potential has the following expression [13, 15, 20, 21]

$$u(\beta) = \left[b^2 - 4a\left(s + \frac{1}{2} + m\right)\right]\beta^2 + 2ab\beta^4 + a^2\beta^6, \tag{2}$$

where, $a > 0$ and b are real parameters, m is a natural number which gives the number of the solutions which are exactly determined, while s is related to ω. According to the Bohr model [1, 2], the energy potential has to depend only on the β and γ deformation variables. Therefore, the quantity $s + 1/2 + m \equiv c$ is forced to remain constant, such that finally one has a state independent potential. This condition is satisfied if the variation of s cancels out the variation of m. Such a mechanism implies a maximal value of m, denoted by k. For example, in the case of the γ-unstable case, by expressing s as a function of τ, one has [13, 21]:

$$(m,\tau) : (k,0),(k-1,2),... \Rightarrow c^{\text{even }\tau}(k) = k + \frac{7}{4}, \tag{3}$$

$$(m,\tau) : (k,1),(k-1,3),... \Rightarrow c^{\text{odd }\tau}(k) = k + \frac{9}{4}. \tag{4}$$

For numerical applications it is more convenient to make the change of variable $\beta = ya^{-1/4}$ and to introduce the notations $\alpha = b/\sqrt{a}$ and $\varepsilon_y = \varepsilon/\sqrt{a}$:

$$\left[-\frac{d^2}{dy^2} + \frac{(\tau+1)(\tau+2)}{y^2} + u^p(y)\right]\eta(y) = \varepsilon_y\eta(y), \text{ where} \tag{5}$$

$$u^p(y) = \left[\alpha^2 - 4c^p(k)\right]y^2 + 2\alpha y^4 + y^6 + u_0^p(k,\alpha),\ p = \text{even}\,\tau, \text{odd}\,\tau, \tag{6}$$

while $u_0^p(k,\alpha)$ are two constants which are set such that the two potentials, for even and odd τ, have the same minimum energy. Eq. (5) is quasi-exactly solved by considering the ansatz function

$$\eta_m(y) \sim P_m(y^2)y^{2s-\frac{1}{2}}e^{-\frac{y^4}{4}-\frac{\alpha y^2}{2}}, \tag{7}$$

which leads to an equation for polynomials in y^2 of order m:

$$\left(-\frac{d^2}{dy^2} - \frac{4s-1}{y}\frac{d}{dy} + 2\alpha\frac{d}{dy} + 2y^3\frac{d}{dy} - 4my^2\right)P_m(y^2) = \lambda P_m(y^2). \tag{8}$$

The total energy of the γ-unstable system is then written as

$$E_{\xi,\tau} = \sqrt{a}\frac{\hbar^2}{2B}\left[\lambda_{\xi,\tau}^{(k)}(\alpha) + \alpha(2\tau+5) + u_0^p(k,\alpha)\right], \tag{9}$$

where B is the mass parameter defining the Bohr Hamiltonian. The scaling factor, is removed if the energies are normalized to the energy of the 2_1^+ state:

$$R_{\xi,\tau} = \frac{E_{\xi,\tau} - E_{1,0}}{E_{1,1} - E_{1,0}},\ \ \xi = 0,1,2,...,k. \tag{10}$$

Finally, the normalized energies depend only on a single free parameter α and on k, respectively on the quantum numbers ξ and τ. By plotting the energy (10) as a function of α within a finite interval, for a fixed k, one can cover a phase transition from a spherical shape to a deformed one, crossing a critical point where the potential is flat [20, 21]. Due to the constraints imposed on the quasi-exact instances of the sextic potential with double minima, it cannot be efficiently applied for the study of the shape coexistence and mixing phenomena. These latter properties are recovered if the conditions imposed on the potential parameters are relaxed and the eigenvalue problem is solved numerically in an appropriate basis. The method is briefly presented in the following.

2.2 Numerical diagonalization method

A general expression of the sextic potential is considered [11] for Eq. (1),

$$v(\beta) = \beta^2 + a\beta^4 + b\beta^6, \tag{11}$$

where a and b are real free parameters. The coefficient of the β^2 is one due to a scaling property of the polynomial potentials which allows to extract one of the parameters as a scaling factor for energies and wave functions. The eigenvalue problem (1) with sextic potential (11) is no more exactly or quasi-exactly solvable and therefore a numerical diagonalization method is applied using as a basis wave functions expressed in terms of Bessel functions of the first kind J_ν,

$$\tilde{\phi}_{\nu n}(\beta) = \frac{\sqrt{2}\beta^{-\frac{3}{2}} J_\nu(z_n^\nu \beta/\beta_w)}{\beta_w J_{\nu+1}(z_n^\nu)}, \tag{12}$$

which are actually solutions of the same Eq. (1), but given instead for an infinite square well potential. The index ν is $\sqrt{L(L+1)/3+9/4}$ and $\tau + 3/2$ for X(5) [7], respectively E(5) [6]. Thus, the total wave function is written as a linear combination in this basis

$$\phi_{\nu\xi}(\beta) = \sum_{n=1}^{n_{Max}} A_{\nu n}^{\xi} \tilde{\phi}_{\nu n}(\beta), \quad \xi = 0, 1, 2, ..., n_{Max}, \tag{13}$$

where n_Max gives the dimension of the basis truncation, while ξ plays the role of the β vibration quantum number. The coefficients $A_{\nu n}^{\xi}$ are determined from the diagonalization of the Hamiltonian matrix:

$$H_{nm} = \left(\frac{z_n^\nu}{\beta_W}\right)^2 \delta_{nm} + \frac{2\sum_{i=1}^{3} q_i \beta_W^{2i} I_{nm}^{(\nu\nu,2i)}}{J_{\nu+1}(z_n^\nu) J_{\nu+1}(z_m^\nu)}, q_1 = 1, q_2 = a, q_3 = b, \tag{14}$$

where

$$I_{nm}^{(\nu\mu,k)} = \int_0^1 x^{k+1} J_\nu(z_n^\nu x) J_\mu(z_m^\mu x) dx, \; x = \beta/\beta_W. \tag{15}$$

This method has been proposed for the first time in [11] and then more closely investigated in [12]. Also, its recent applications for experimental data [12,22,23] confirmed that shape coexistence and mixing phenomena are now appropriately addressed. Concerning the calculations of the $B(E2)$ transitions, in both methods, a harmonic quadrupole transition operator is used by taking into account the contributions coming from the matrix elements for the γ variable and the Euler angles describing the rotations:

$$T_{\mu}^{(E2)} = t\beta \left[D_{\mu,0}^{2} \cos\gamma + \frac{\sin\gamma}{\sqrt{2}} \left(D_{\mu,2}^{2} + D_{\mu,-2}^{2} \right) \right]. \tag{16}$$

Another important observable, which is often considered a signature [8] for shape coexistence and mixing, is the monopole transition $\rho_{i,f}^{2} \sim \langle i|\beta^{2}|f\rangle^{2}$, calculated usually [11] between the first excited 0_{2}^{+} and the ground state 0_{1}^{+}.

3 Numerical Results and Application to Experimental Data

Recently, the quasi-exactly solvable sextic potential (6) has been applied for γ-unstable nuclei [21] looking for the influence of the solvability order k on the structure of the states along the shape phase transition and especially in its critical point. As a reference for this study has been taken the previous work [14], where only $k = 1$ was considered in analyzing the isotope chains of Ru, Pd and Cd. The same isotope chains have been investigated also in [21], but for $k > 1$, reaching a different conclusion concerning the characteristic of the shape phase transition and the selection of the best candidate nuclei for the critical point as can be seen here from Figure 1. Thus, according to $k = 1$ [14] there is no phase transition from spherical vibrator to γ-unstable shape for the isotope chains of Pd and Cd, which is not the case in Figure 1, if one considers $k > 1$. For example, within the isotope chain of Cd one has a phase transition from a deformed shape (small α) to a spherical one (large α) crossing the critical point (dashed lines) close to ^{108}Cd for all four values of $k > 1$. In the case of the isotopes of Pd, one has multiple crossing of the horizontal dashed line, with ^{104}Pd and ^{110}Pd as good candidates for the critical point. For Ru, both $k = 1$ and $k > 1$ predict a similar shape phase transition, but giving different candidates for the critical point, with ^{104}Ru for $k = 1$ [14] and ^{100,102}Ru [21] for $k > 1$. An explanation for these discrepancies between $k = 1$ and $k > 1$ is that the number of eigenstates, which can be exactly determined for $k = 1$, are not enough to cover all the available experimental data as is the case of $k > 1$. Nevertheless, some small differences are even between values of $k > 1$ concerning the energy ratios $E(4_{1}^{+})/E(2_{1}^{+})$ and $E(0_{2}^{+})/E(2_{1}^{+})$ [21], especially in the critical point, which explain why the candidates for the critical point prefer more a value of k than other. For example, ^{100,102}Ru are much closer to the critical point corresponding to $k = 5$ than the other values considered in Figure 1. In Figure 2, are shown energy spectra and $B(E2)$ transitions for ^{102}Ru$(= 5)$, ^{104}Pd$(k = 10)$

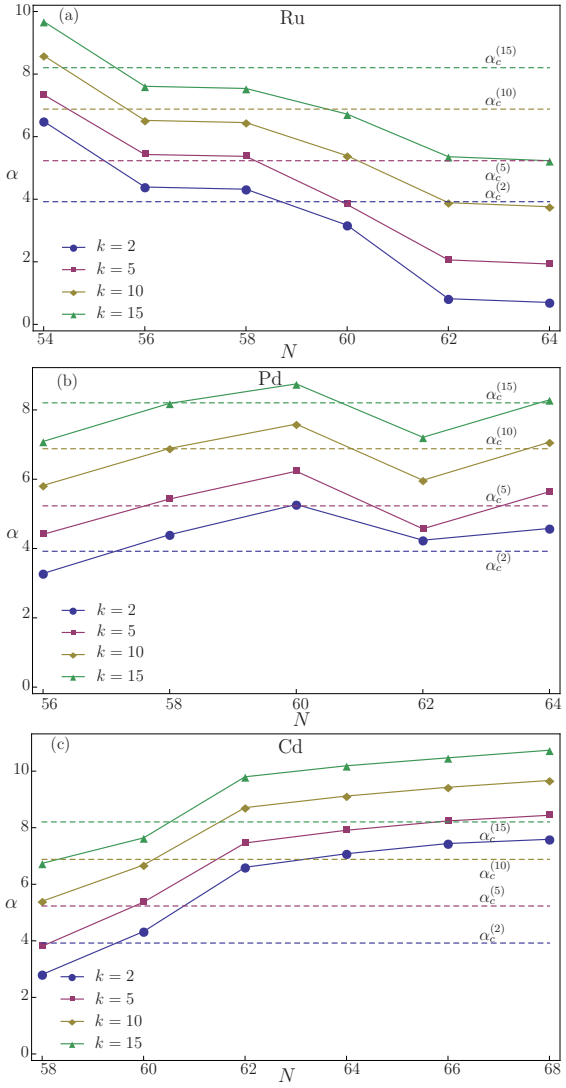

Figure 1. The free parameter α as a function of the neutron number N for isotopes of Ru (a), Pd (b) and Cd (c), when $k = 2$, 5, 10 and 15. The full lines indicate the shape evolution within the isotope chain, while the horizontal dashed ones are for the critical points $\alpha_c^{(2)} = 3.92$, $\alpha_c^{(5)} = 5.23$, $\alpha_c^{(10)} = 6.88$ and $\alpha_c^{(15)} = 8.20$, respectively.

and ^{108}Cd($k = 5$), which are the best candidates for the critical point, by selecting that value of k for which these nuclei are closer to the horizontal dashed line.

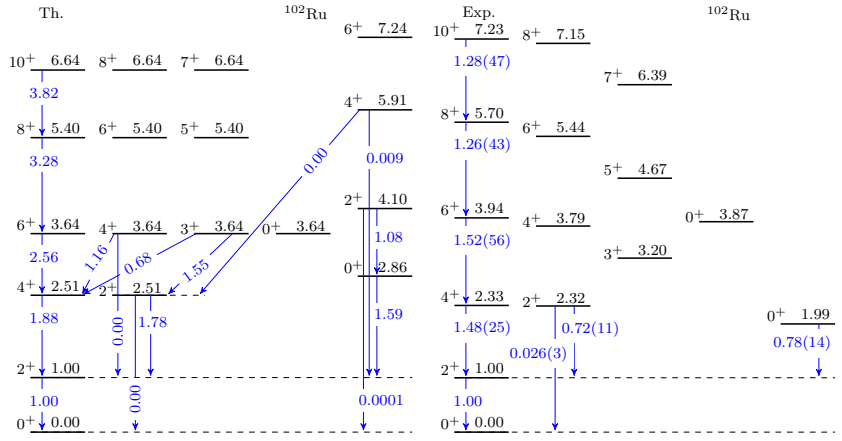

Figure 2. Energy spectra and $B(E2)$ transitions for $k = 5$ are compared with experimental data of ^{102}Ru [24].

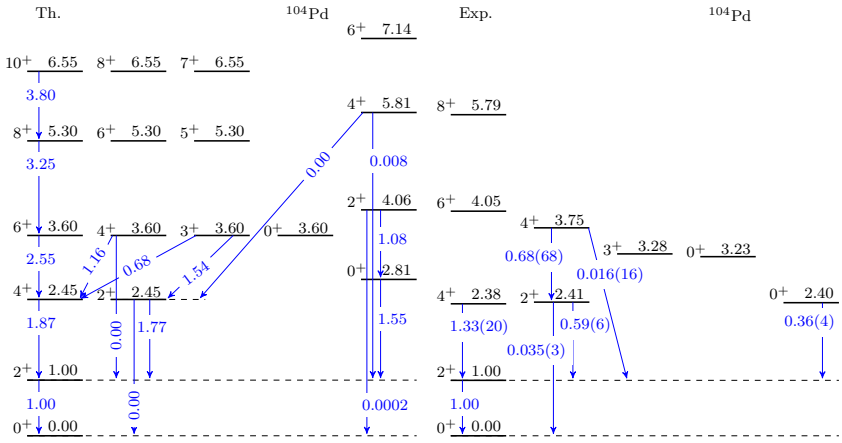

Figure 3. The same as in Figure 2, but for ^{104}Pd [25] and $k = 10$.

The agreement between theory and experiment is good in average taking in consideration that a single free parameter is involved in the fitting procedure, while the experimental data correspond to three bands plus an extra 0^+ state. Also, due to O(6) symmetry, within this model some states are degenerated, which is not the case in experiment. Some improvements of the model are possible by introducing an SO(5) conserving term $\hat{L}^2$ [23], which splits these degenerated states without affecting the wave functions, respectively by considering anaharmonic terms [16, 17] for the transition operator (16). An overall conclusion regarding the quasi-exactly solvable sextic potential, based on all its applications made

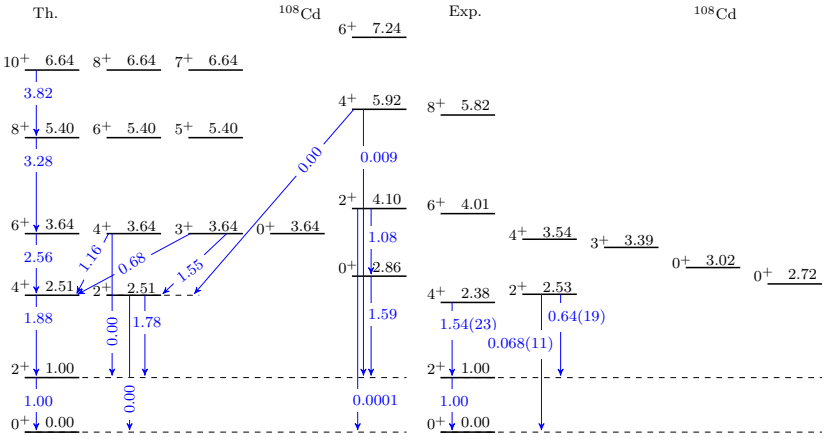

Figure 4. The same as in Figure 2, but for ^{108}Cd [26] and $k = 5$.

for the Bohr model, is that it is suitable to describe shape phase transitions and critical point having also the advantage of offering analytical expressions for energies and wave functions. Other phenomena, as dynamical shape evolution, shape coexistence and mixing cannot be described within this model and are more appropriately addressed if a general sextic potential (11) is involved, as it has been already discussed in the previous section. By letting free all the parameters of the sextic potential, a barrier can be introduced in the critical point. In other words, in the absence of the barrier or for a very small barrier, one has shape fluctuations describing the critical points [6, 7], while for a considerable height of the barrier, one has shape coexistence and mixing as it is illustrated in Figure 5. For example, in Figure 5(a), for a very high barrier, the density probability distribution has a single peak centered around the less deformed minimum for the first excited 0^+ state, respectively a single peak localized around the more deformed minimum for the ground state. The two 0^+ states are closer in energy and the lowest states built on them are almost completely separated without manifesting a β vibration motion and thus behaving like being in competition for the ground band. Corroborating these features with the small value for the monopole transition, one has the picture for what is defined in literature [8] as shape coexistence phenomenon in nuclei. On the other hand, by decreasing the barrier, as in Figure 5(b), the two configuration states start to interact due to the tunneling of the barrier giving birth to the shape coexistence and mixing phenomena. This is clearly reflected in the fact that the density distribution probability has now two peaks, one for each minimum, but also in a large value of the monopole transition.

Thus, once with the introduction of the barrier, new possible applications of the Bohr Hamiltonian emerged, namely in the topic of shape coexistence and

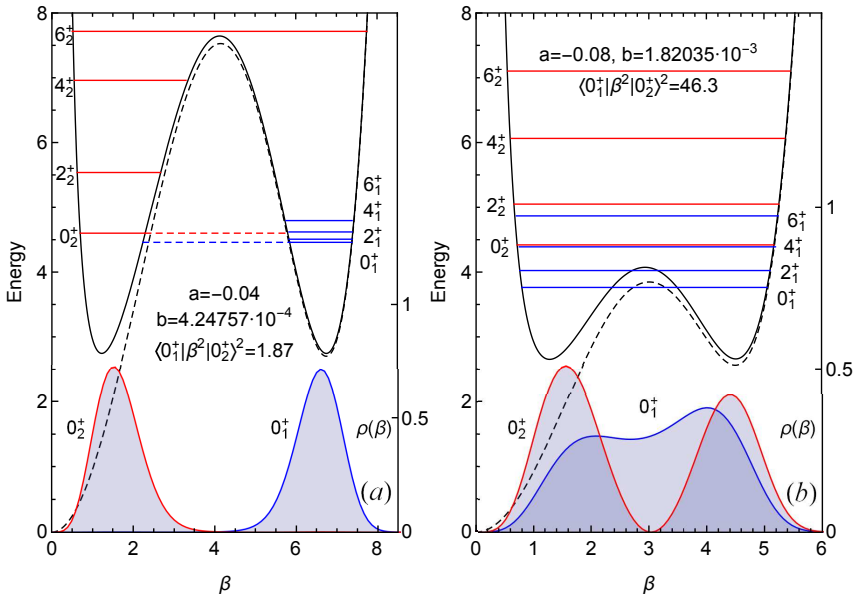

Figure 5. Plots of the energy potential $v(\beta)$ (11) (dashed curve) and of the effective potential $v(\beta) + \omega/\beta^2$ (full curve), as well as of the density distribution probability $\rho(\beta) = |\phi|^2\beta^4$ for the ground state (0_1^+) and first excited 0_2^+ state, are given for a high barrier (a), respectively a moderate one (b). On the same panels are also indicated the values for the monopole transition $\langle 0_1^+|\beta^2|0_2^+\rangle^2$ and for the parameters a and b defining the potential.

mixing phenomena. The model has been already applied with success in ^{76}Kr [12], ^{72,74,76}Se [22] and ^{96,98,100}Mo [23] nuclei, known for manifesting such behavior. Due to the lack of space, we limit ourselves only to attract the attention on these results here.

4 Conclusions

In Ref. [21], for the Bohr Hamiltonian with sextic potential [15], it was evidenced more clearly the importance had by the solvability order k on the structure of the states along the shape phase transition and especially on its critical point. Comparing the $k = 1$ [14] and $k > 1$ [21] cases, it was evidenced that one has to consider at least $k = 2$ in order to have a realistic description of the available experimental data. Moreover, in [11, 12] it is shown that by solving numerically the eigenvalue problem instead of quasi-exactly, phenomena as shape coexistence and mixing can be described by introducing a barrier which separates the spherical shape by the deformed one. The predicting ability of model [11] has been already confirmed by its recent applications [12, 22, 23]

for several nuclei suspected for shape coexistence and mixing. In this form, the model is more suitable to describe shape coexistence and mixing between an approximately spherical shape and a deformed one and therefore new applications can be done for other nuclei which are candidates for this picture. On the other hand, the model can be further developed by considering an octic potential, which would allow a description of a shape coexistence between two well deformed shapes. Also, one can include triaxial deformation or γ-rigidity, getting more possible situations for shape coexistence and mixing, which could cover more experimental data.

Acknowledgements

Work supported by PN 19 06 01 01/2019, Ministry of Research and Innovation.

References

[1] A. Bohr (1952) *Mat. Fys. Medd. Dan. Vid. Selsk.* **26** No. 14
[2] A. Bohr, B. R. Mottelson (1953) *Mat. Fys. Medd. Dan. Vid. Selsk.* **27** No. 16
[3] J. H. Ginocchio, M. W. Kirson (1980) *Phys. Rev. Lett.* **44** 1744
[4] A. E. L. Dieperink, O. Scholten, F. Iachello (1980) *Phys. Rev. Lett.* **44** 1747
[5] R. F. Casten (2006) *Nature Phys.* **2** 820
[6] F. Iachello (2000) *Phys. Rev. Lett.* **85** 3580
[7] F. Iachello (2001) *Phys. Rev. Lett.* **87** 052502
[8] K. Heyde, J. L. Wood (2011) *Rev. Mod. Phys.* **83** 1467
[9] L. Fortunato (2005) *Eur. Phys. J. A* **26** 1-30
[10] P. Buganu, L. Fortunato (2016) *J. Phys. G: Nucl. Part. Phys.* **43** 093003
[11] R. Budaca, P. Buganu, A.I. Budaca (2018) *Phys. Lett. B* **776** 26-31
[12] R. Budaca, A.I. Budaca (2018) *EPL* **123** 42001
[13] G. Lévai, J.M. Arias (2004) *Phys. Rev. C* **69** 014304
[14] G. Lévai, J.M. Arias (2011) *Phys. Rev. C* **81** 044304
[15] A.G. Ushveridze (1994) "*Quasi-exactly solvable models in quantum mechanics*". IOP, Bristol pp. 82–94.
[16] A.A. Raduta, P. Buganu (2011) *Phys. Rev. C* **83** 034313
[17] A.A. Raduta, P. Buganu (2013) *J. Phys. G: Nucl. Part. Phys.* **40** 025108
[18] P. Buganu, R. Budaca (2015) *Phys. Rev. C* **91** 014306
[19] P. Buganu, R. Budaca (2015) *J. Phys. G: Nucl. Part. Phys.* **42** 105106
[20] R. Budaca, P. Buganu, M. Chabab, A. Lahbas, M. Oulne (2016) *Ann. Phys. (NY)* **375** 65-90
[21] A. Lahbas, P. Buganu, R. Budaca under review
[22] R. Budaca, P. Buganu, A.I. Budaca (2019) *Nucl. Phys. A* **990** 137-148
[23] R. Budaca, A.I. Budaca, P. Buganu (2019) *J. Phys. G: Nucl. Part. Phys.* **46** 125102
[24] D. De Frenne (2009) *NDS* **110** 1745
[25] J. Blachot (2007) *NDS* **108** 2035
[26] J. Blachot (2008) *ENSDF*